Supporting Information

Crystal engineering and sorption studies on CN- and dipyridyl-bridged 2D coordination polymers

Valoise Brenda Nguepmeni Eloundou[a,b] , Patrice Kenfack Tsobnang*[a], Theophile Kamgaing[a], Chiranjib Gogoi [b], Nieves Lopez-Salas[c], Susan A. Bourne*[b]

[a] Department of Chemistry, University of Dschang, PO Box 67, Dschang, Cameroon

[b] Centre for Supramolecular Chemistry Research, University of Cape Town, Rondebosch 7701, South Africa

[c] Sustainable Materials Chemistry, Department of Chemistry, Paderborn University, Warburger Str. 100, 33098, Paderborn, Germany

Corresponding Authors:

Prof. Susan Bourne: susan.bourne@uct.ac.za

A/Prof. Patrice Kenfack Tsobnang: pakenfack@gmail.com, patrice.kenfack@univ-dschang.org

Additional Emails: eloundoubrenda@gmail.com , theokamgaing@yahoo.fr, nieves.lopez.salas@uni-paderborn.de, chiranjib.gogoi@uct.ac.za.

Section 1: Synthesis of $K_2[Ni(CN)_4]\cdot H_2O$

$K_2[Ni(CN)_4]\cdot H_2O$ was prepared as reported in previous works [1-3], by mixing stoichiometric amounts of nickel(II) chloride hexahydrate with potassium cyanide in water solution. To 10 mL aqueous solution of $NiCl_2\cdot 6H_2O$ (0.238 g, 1 mmol) was added a 10 mL aqueous solution of KCN (0.13 g, 2 mmol). The grayish green precipitate of nickel cyanide $[Ni(CN)_2]$ was washed carefully with hot water (100°C) to remove the impurities. $[Ni(CN)_2]$ was then dissolved in 10 ml aqueous solution of KCN (0.13 g, 2 mmol).The orange obtained solution was filtered and kept at room temperature for crystallization, and yellow $K_2[Ni(CN)_4]\cdot H_2O$ crystals were obtained after few days.

Section 2: Characterisation of 1 and 2

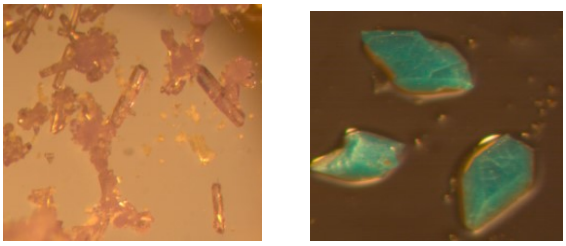

(a) (b)

Figure S1. Microscopic picture of **1** (a) and microscopic picture of **2** (b).

Infrared spectroscopy

The symmetric C^{sp2}–H (-CH_2) stretching vibrations appear at 2940 cm^{-1} in **1** or at 2938 cm^{-1} in **2**. We also note the presence of the adsorption band at 2165 cm^{-1} (for **1)** or at 2135 cm^{-1} (for **2**) which can be related to the vibration mode of C≡N which in the literature appears between 2000-2200 cm^{-1} [4-5] We also note the presence of the adsorption band at 1614 cm^{-1} (for **1**) or at 1616 cm^{-1} (for **2)** characteristic of the vibration mode of the C=N [6] This band could be also assigned to the deformation vibration mode of OH which in the literature appears at 1614 cm^{-1}. The adsorption band at 1560 cm^{-1} which appears in both spectra is characteristic of the vibration mode of C=C group of 1,2-bis(4-pyridyl)ethane ligand. The presence of the adsorption band at 1424 cm^{-1} can be assigned to the bending vibrational mode of the C-H bond of this ligand. The band at 1358 cm^{-1} can be attributed to stretching vibrations of ν(C−C, C−N) [6] The presence of the adsorption band at 1020 cm^{-1} can be assigned to the CH_2 wagging vibration mode of 1,2-bis(4-pyridyl)ethane [7]]. The band at 834 cm^{-1} is assigned to aromatic ring vibration. The presence of the adsorption band at 550 or at 547cm^{-1} can be assigned to the vibrational mode of the Ni-N bond. It appears from this infrared spectroscopic analysis that the 1,2-bis(4-pyridyl)ethane ,cyanide and water molecules are present in **1** and **2.**

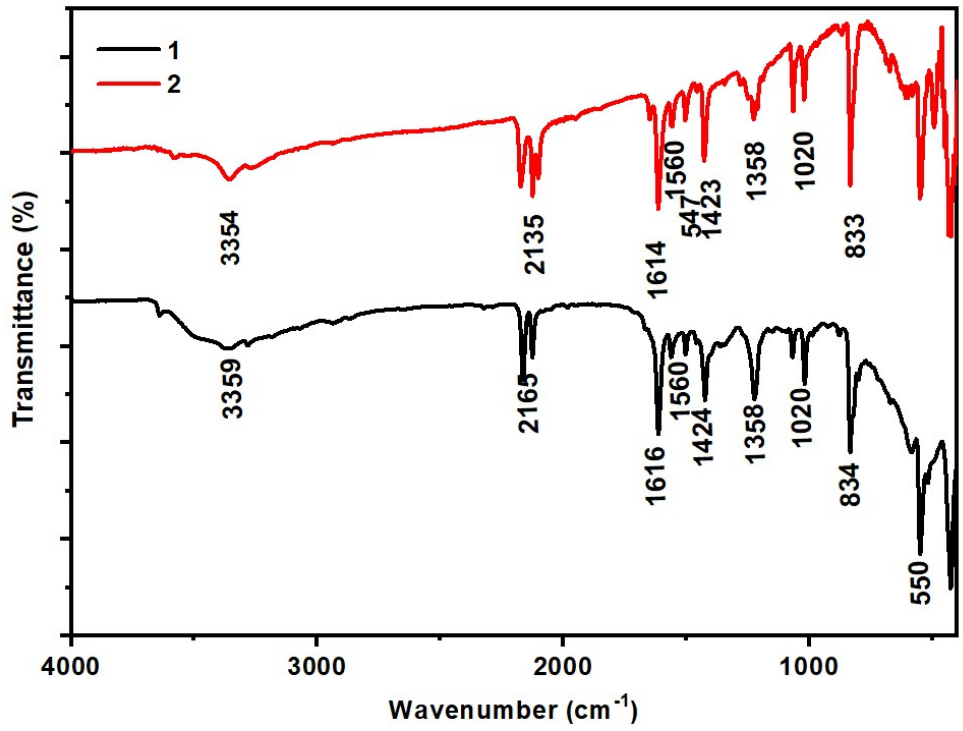

Figure S2. FTIR spectrum of **1 (black) and 2 (red).**

Table S1. Summary of the assignment of the characteristic frequencies observed in the FTIR spectra of **1** and **2.**

Frequencies bands (cm^{-1}) of 1	Frequencies bands (cm^{-1}) of 2	Assigned vibrations
3359	3354	ϒO-H
2940	2938	ϒCH_2
2165	2135	ϒC≡N
1614	1616	ϒC=N or δO-H
1560	1560	ϒC=C
1424	1423	δC-H
1358	1358	ϒ(C−C,C−N)
1020	1060-1020	CH_2 wagging
834	833	Aromatic ring
550	547	ϒM-N

ϒ : stretching ; δ : bending

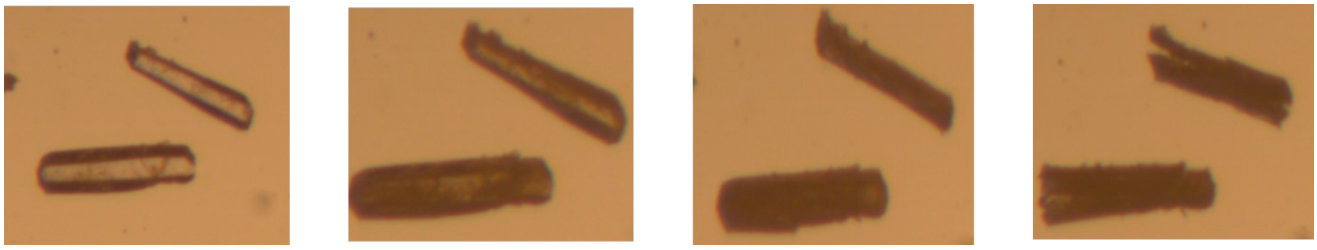

a b c d

Figure S3. HSM images of **1** at (a) 21 ℃, (b) 73 ℃, (c) 80 ℃, (d) 100-300 ℃.

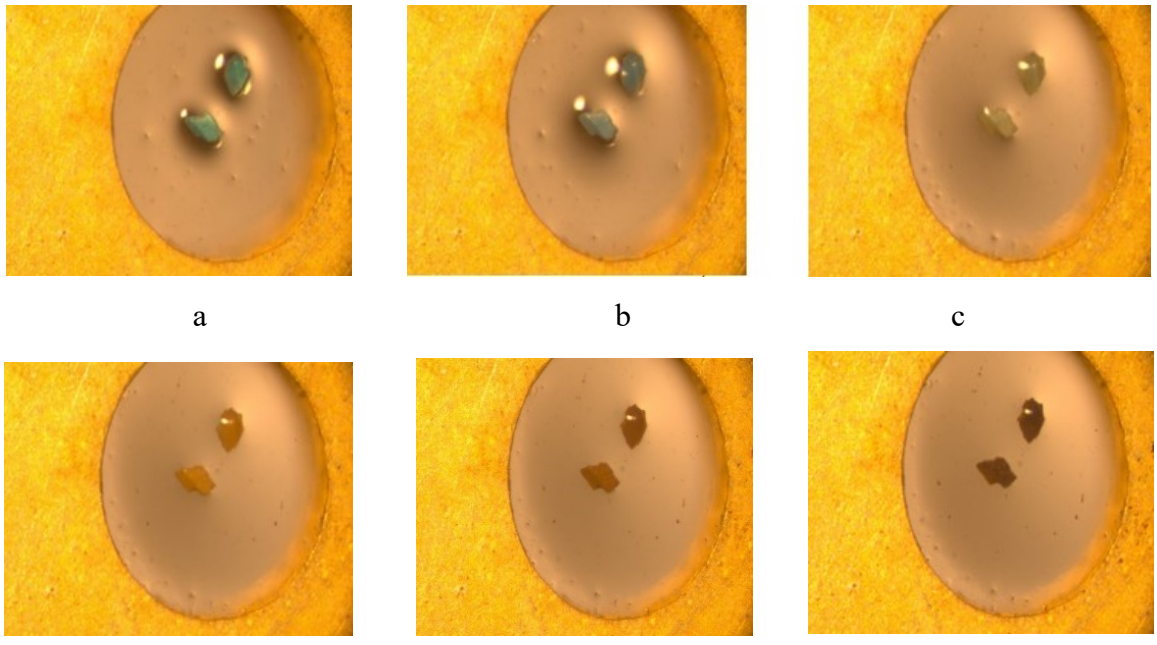

a b c

d e f

Figure S4. HSM images of **2** at (a) 26 ℃, (b) 100 ℃, (c) 245 ℃, (d) 300℃, (e) 320 ℃ and (f) 330 ℃.

UV-Visible absorption analysis

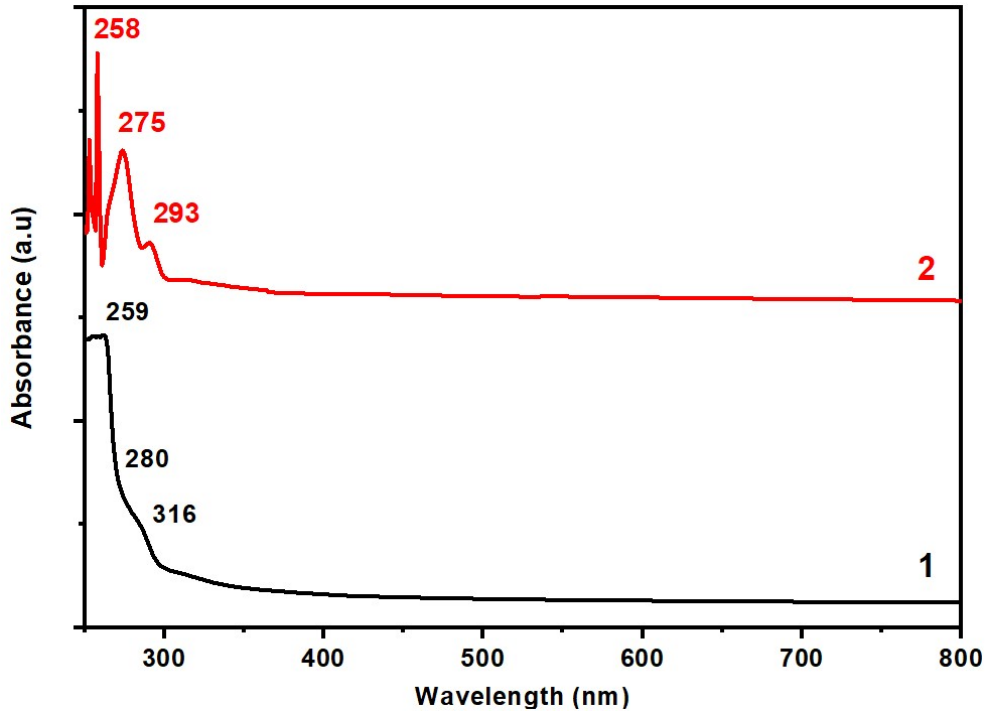

Figure S5. UV-Vis spectrum of **1** and **2**

The UV-Visible absorption spectrum of **1** and **2** (Figure S5) contains three absorption bands (259 nm, 280 nm and 316 nm for **1** and 258 nm, 275 nm and 293nm for **2**). The two first one at 259 nm and 280 nm for **1** (or 258 nm and 275 nm for **2**) observed in the ultraviolet region of the spectrum could be attributed to n→π*electronic transition of 1,2-bis(4-pyridyl)ethane ligand. The third band at 316 nm for **1** (or 293 nm for **2**) denotes the presence of Ni atom in a square planar geometry and to the ligand field transitions, namely $^{1}A_1 \rightarrow {}^{1}T_1$ in $[Ni^{II}(CN)_4]^{2-}$ [8] .

Table S2. Bond distances (Å) for **1**

Atom	Atom	Length/Å	Atom	Atom	Length/Å
$Ni_{(1)}$	$N_{(3)}$	2.125(2)	$Ni_{(2)}$	$C_{(1C)}{}^{2}$	1.907(10)
$Ni_{(1)}$	$N_{(3)}{}^{1}$	2.124(2)	$N_{(3)}$	$C_{(6)}$	1.344(4)
$Ni_{(1)}$	$O_{(1)}$	2.103(2)	$N_{(3)}$	$C_{(3)}$	1.342(4)
$Ni_{(1)}$	$O_{(1)}{}^{1}$	2.103(2)	$N_{(2)}$	$C_{(2)}$	1.151(4)
$Ni_{(1)}$	$N_{(2)}$	2.051(2)	$C_{(6)}$	$C_{(7)}$	1.383(4)
$Ni_{(1)}$	$N_{(2)}{}^{1}$	2.051(2)	$C_{(3)}$	$C_{(4)}$	1.377(4)
$Ni_{(2)}$	$C_{(2)}$	1.852(3)	$C_{(5)}$	$C_{(7)}$	1.385(4)
$Ni_{(2)}$	$C_{(2)}{}^{2}$	1.852(3)	$C_{(5)}$	$C_{(4)}$	1.384(4)
$Ni_{(2)}$	$C_{(1B)}{}^{2}$	1.807(16)	$C_{(5)}$	$C_{(8)}$	1.506(4)
$Ni_{(2)}$	$C_{(1B)}$	1.807(16)	$C_{(8)}$	$C_{(8)}{}^{3}$	1.549(6)
$Ni_{(2)}$	$C_{(1A)}{}^{2}$	1.900(12)	$C_{(1B)}$	$N_{(1B)}$	1.186(19)
$Ni_{(2)}$	$C_{(1A)}$	1.900(12)	$N_{(1A)}$	$C_{(1A)}$	1.130(14)
$Ni_{(2)}$	$C_{(1C)}$	1.907(10)	$N_{(1C)}$	$C_{(1C)}$	1.127(12)
$O_{(1)}$	$H_{(1A)}$	0.980(17)	$O_{(1)}$	$H_{(1B)}$	0.997(17)
$C_{(3)}$	$H_{(3)}$	0.9500	$C_{(6)}$	$H_{(6)}$	0.9500
$C_{(4)}$	$H_{(4)}$	0.9500	$C_{(8)}$	$H_{(8A)}$	0.9900
$C_{(8)}$	$H_{(8B)}$	0.9900			

[1]1-X,1-Y,-Z; [2]-X,2-Y,-Z; [3]2-X,1-Y,1-Z

Table S3. Bond angles (°) for 1

Atom	Atom	Atom	Angle/°	Atom	Atom	Atom	Angle/°
$N_{(3)}{}^{1}$	$Ni_{(1)}$	$N_{(3)}$	180.0	$C_{(1B)}$	$Ni_{(2)}$	$C_{(2)}$	90.4(5)
$O_{(1)}$	$Ni_{(1)}$	$N_{(3)}$	90.82(9)	$C_{(1B)}{}^{2}$	$Ni_{(2)}$	$C_{(2)}$	89.6(5)
$O_{(1)}{}^{1}$	$Ni_{(1)}$	$N_{(3)}{}^{1}$	90.84(9)	$C_{(1B)}{}^{2}$	$Ni_{(2)}$	$C_{(1C)}{}^{2}$	10.8(7)
$O_{(1)}$	$Ni_{(1)}$	$N_{(3)}{}^{1}$	89.16(9)	$C_{(1B)}$	$Ni_{(2)}$	$C_{(1C)}{}^{2}$	169.2(7)
$O_{(1)}{}^{1}$	$Ni_{(1)}$	$N_{(3)}$	89.18(9)	$C_{(1A)}{}^{2}$	$Ni_{(2)}$	$C_{(1A)}$	180.0
$O_{(1)}{}^{1}$	$Ni_{(1)}$	$O_{(1)}$	180.0	$C_{(1A)}$	$Ni_{(2)}$	$C_{(1C)}{}^{2}$	159.1(6)
$N_{(2)}$	$Ni_{(1)}$	$N_{(2)}{}^{1}$	180.0	$N_{(2)}$	$C_{(2)}$	$Ni_{(2)}$	179.1(2)

$C_{(2)}{}^{2}$	$Ni_{(2)}$	$C_{(2)}$	180.00(18)	$N_{(1B)}$	$C_{(1B)}$	$Ni_{(2)}$	178.1(16)
$N_{(2)}{}^{1}$	$Ni_{(1)}$	$O_{(1)}$	91.24 (9)	$N_{(2)}$	$Ni_{(1)}$	$O_{(1)}$	88.76 (9)
$N_{(2)}{}^{1}$	$Ni_{(1)}$	$O_{(1)}{}^{1}$	88.76 (9)	$N_{(2)}{}^{1}$	$Ni_{(1)}$	$O_{(1)}{}^{1}$	91.24 (9)
$N_{(2)}{}^{1}$	$Ni_{(1)}$	$N_{(3)}{}^{1}$	89.70 (9)	$N_{(2)}$	$Ni_{(1)}$	$N_{(3)}{}^{1}$	90.30 (9)
$N_{(2)}{}^{1}$	$Ni_{(1)}$	$N_{(3)}$	90.30 (9)	$N_{(2)}$	$Ni_{(1)}$	$N_{(3)}$	89.70 (9)
$O_{(1)}$	$Ni_{(1)}$	$N_{(3)}$	89.16(9)	$N_{(3)}{}^{1}$	$Ni_{(1)}$	$N_{(3)}$	180.0
$C_{(1B)}{}^{2}$	$Ni_{(2)}$	$C_{(1B)}$	180.0	$C_{(2)}$	$Ni_{(2)}$	$C_{(1A)}$	93.4(4)
$C_{(2)}{}^{2}$	$Ni_{(2)}$	$C_{(1A)}{}^{2}$	93.4(4)	$C_{(2)}$	$Ni_{(2)}$	$C_{(1A)}{}^{2}$	86.6(4)
$C_{(2)}{}^{2}$	$Ni_{(2)}$	$C_{(1A)}$	86.6(4)	$C_{(2)}{}^{2}$	$Ni_{(2)}$	$C_{(1C)}$	91.9(3)
$C_{(2)}$	$Ni_{(2)}$	$C_{(1C)}$	88.1(3)	$C_{(2)}{}^{2}$	$Ni_{(2)}$	$C_{(1C)}{}^{2}$	88.1(3)
$C_{(2)}$	$Ni_{(2)}$	$C_{(1C)}{}^{2}$	91.9(3)	$C_{(1A)}{}^{2}$	$Ni_{(2)}$	$C_{(1C)}{}^{2}$	20.9(6)

[1]1-X,1-Y,-Z; [2]-X,2-Y,-Z

Table S4. Bond distances (Å) for **2**

Atom	Atom	Length/Å	Atom	Atom	Length/Å
Cu1	$N3^{1}$	2.058(2)	N2	C2	1.153(3)
Cu1	N3	2.058(2)	C4	C7	1.385(3)
Cu1	O1	2.030(2)	C4	C3	1.388(3)
Cu1	$O1^{1}$	2.030(2)	C7	C6	1.391(4)
Cu1	$N2^{1}$	2.438(2)	C7	C8	1.510(3)
Cu1	N2	2.438(2)	C6	C5	1.384(3)
Ni1	$C1^{2}$	1.870(3)	N1	C1	1.149(4)
Ni1	C1	1.870(3)	C8	$C8^{3}$	1.537(5)
Ni1	$C2^{2}$	1.870(3)	C10	C9	1.277(18)
Ni1	C2	1.870(3)	C10	O2	1.580(19)
N3	C5	1.344(3)	C10	O3	1.356(19)
N3	C3	1.343(3)	O3	$O3^{5}$	1.33(3)
O1	H1A	0.993(17)	O1	H1B	0.90(2)
C4	H4	0.88(3)	C6	H6	0.9500

C5	H5	0.97(3)	C3	H3	0.95(3)
C8	H8A	0.9900	C8	H8B	0.9900
C10	C9[4]	2.012(13)	C9	C9[4]	1.889(17)

[1]1-X,-Y,1-Z; [2]2-X,1-Y,1-Z; [3]-X,1-Y,2+Z; [4]1-X,-Y,2-Z ; [5]2- X,-Y,2+Z

Table S5. Bond angles (°) for **2**

Atom	Atom	Atom	Angle/°	Atom	Atom	Atom	Angle/°
N3[1]	Cu1	N3	180.0	C2[2]	Ni1	C2	180.0
N3	Cu1	N2[1]	90.10(8)	C5	N3	Cu1	119.79(17)
N3[1]	Cu1	N2	89.90(8)	C3	N3	Cu1	122.39(16)
N3[1]	Cu1	N2[1]	90.10(8)	C3	N3	C5	117.7(2)
N3	Cu1	N2	90.10(8)	C2	N2	Cu1	157.6(2)
O1	Cu1	N3[1]	90.17(9)	C7	C4	C3	119.8(2)
O1	Cu1	N3	89.83(9)	C4	C7	C6	117.3(2)
O1[1]	Cu1	N3	90.17(9)	C4	C7	C8	122.4(2)
O1[1]	Cu1	N3[1]	89.83(9)	C6	C7	C8	120.2(2)
O1	Cu1	O1[1]	180.0	C5	C6	C7	119.8(2)
O1	Cu1	N2[1]	88.16(9)	N3	C5	C6	122.6(2)
O1	Cu1	N2	91.84(9)	N3	C3	C4	122.6(2)
O1[1]	Cu1	N2	88.16(9)	N1	C1	Ni1	177.9(2)
O1[1]	Cu1	N2[1]	91.84(9)	N2	C2	Ni1	178.4(2)
N2	Cu1	N2[1]	180.00(8)	C7	C8	C8[3]	110.6(2)
C1[2]	Ni1	C1	180.0	C9	C10	O2	133.4(9)
C1	Ni1	C2	89.43(11)	C9	C10	O3	160.6(9)
C1[2]	Ni1	C2	90.57(11)	C10	C9	C10[4]	114.3(8)
C1[2]	Ni1	C2[2]	89.43(11)	C1	Ni1	C2[2]	90.57(11)

[1]1-X,-Y,1-Z; [2]2-X,1-Y,1-Z; [3]-X,1-Y,2+Z; [4]1-X,-Y,2-Z ; [5]2- X,-Y,2+Z

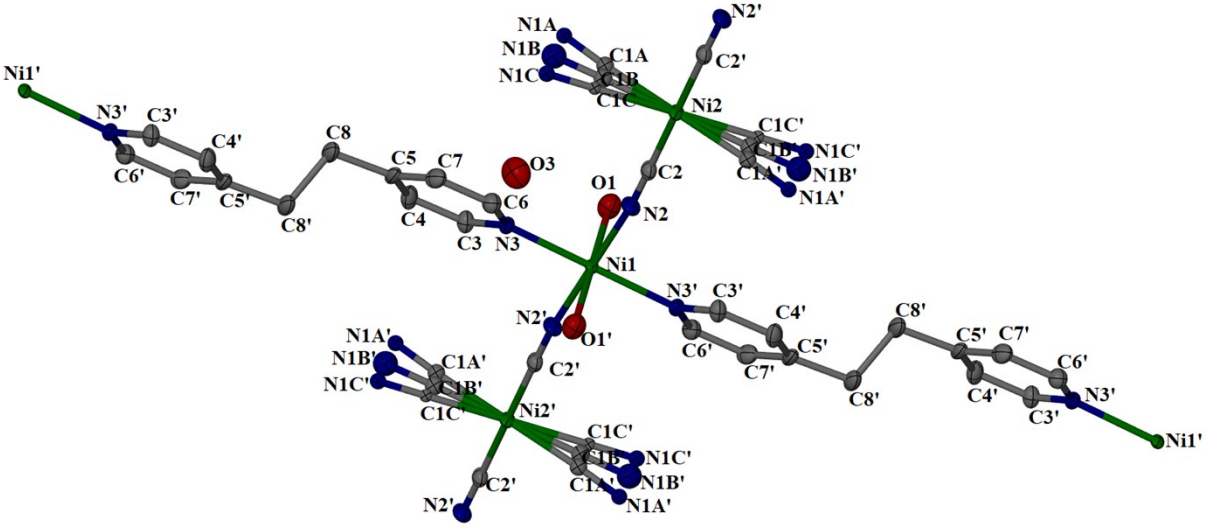

Figure S6. A basic motif of **1**, with total labeling scheme provided. All hydrogens were omitted for clarity.

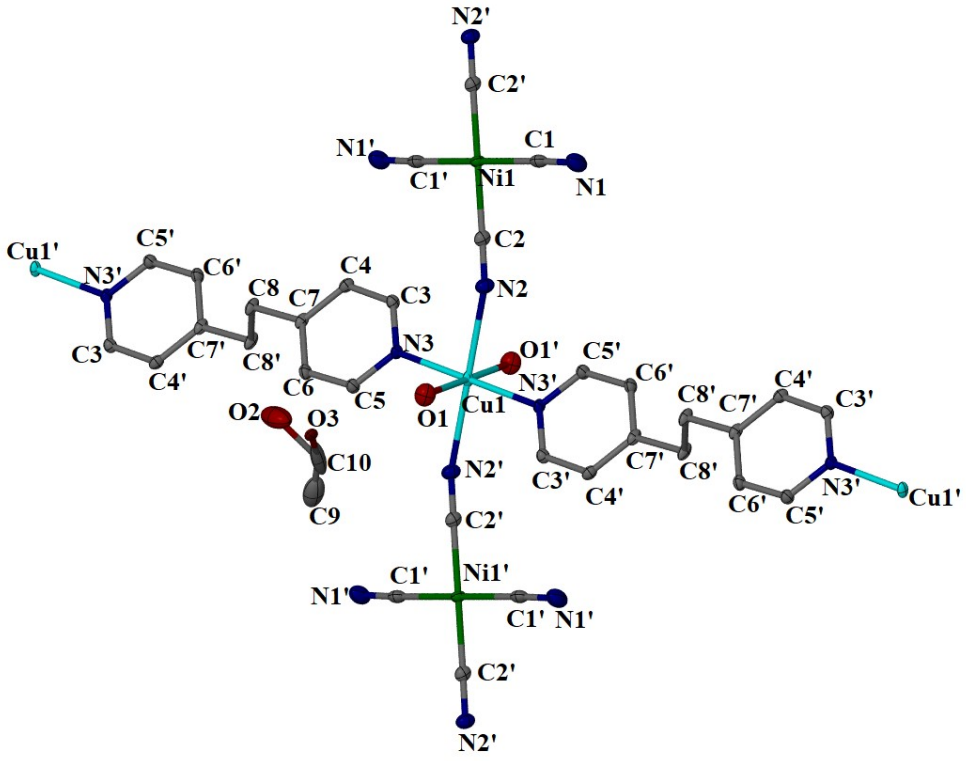

Figure S7. A basic motif of **2** molecules, with total labeling scheme provided. All hydrogens were omitted for clarity.

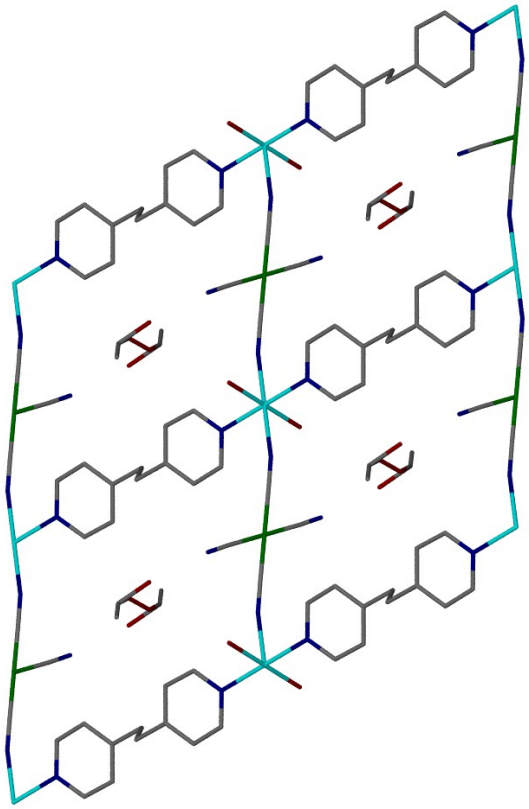

Figure S8. 2-periodic framework of **2** (green – Ni, cyan– Cu, blue – N, grey – C, red-O)

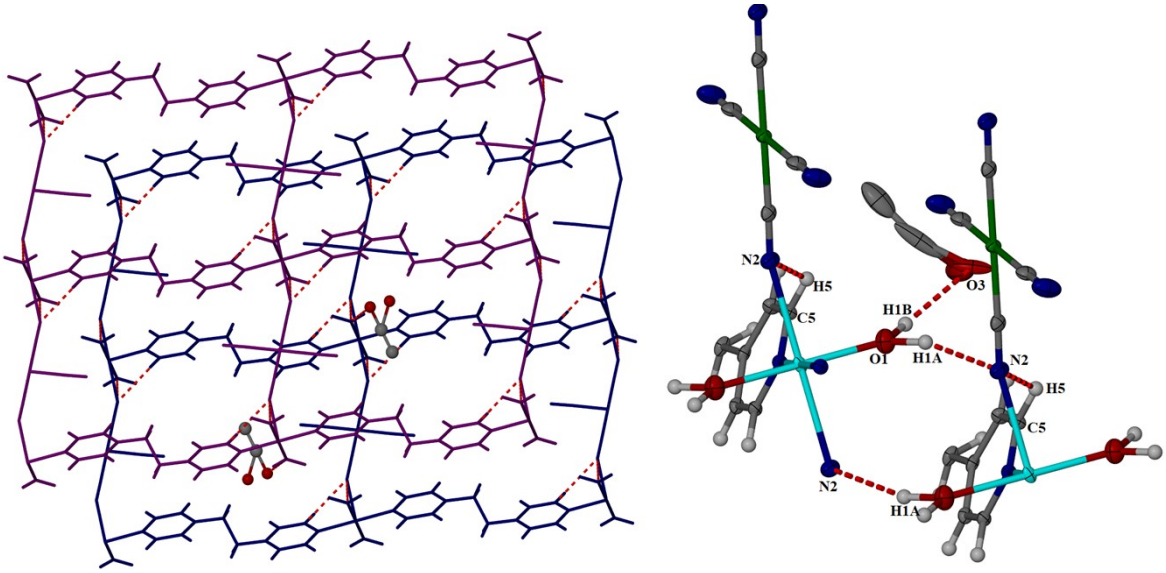

(a) **(b)**

Figure S9. Bilayers and hydrogen bonds in **2 (a** and **b)** formed by 2 separated neighboring 2-periodic frameworks through the hydrogen bonds. All hydrogens and crystallization waters were omitted for clarity.

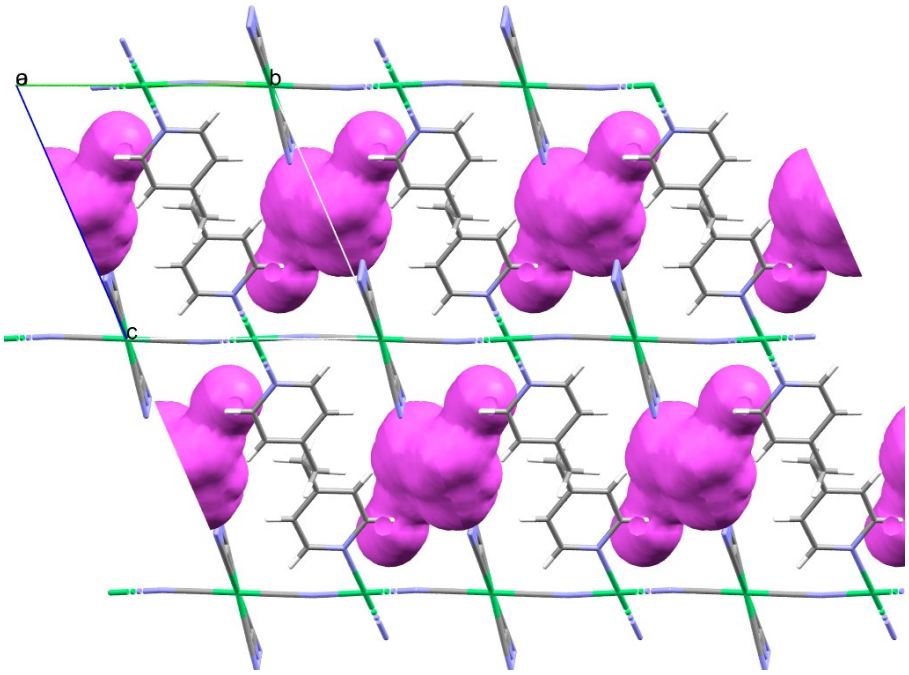

Figure S10. Potential void spaces without solvent molecules (coordinated and uncoordinated) in compound **1** as viewed along the a-axis directions.

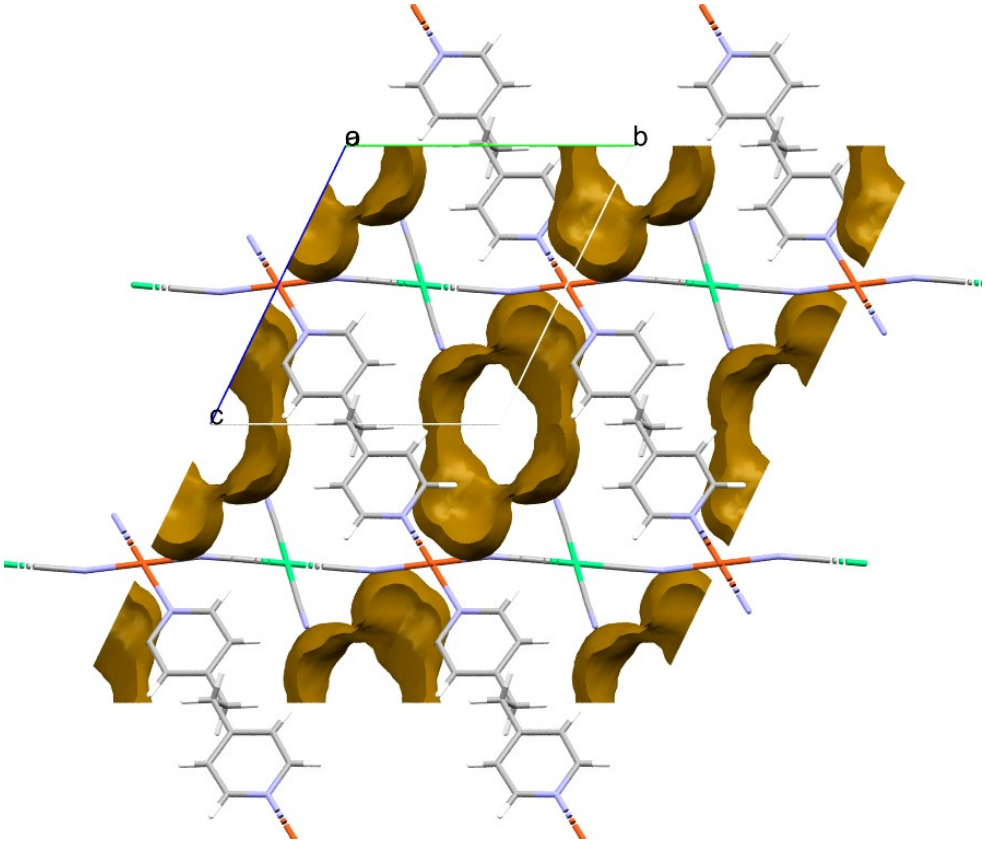

Figure S11. Potential void spaces without solvent molecules (coordinated and uncoordinated) in compound **2** as viewed along the a-axis directions.

Variable-temperature powder X-ray diffraction of 1 and 2

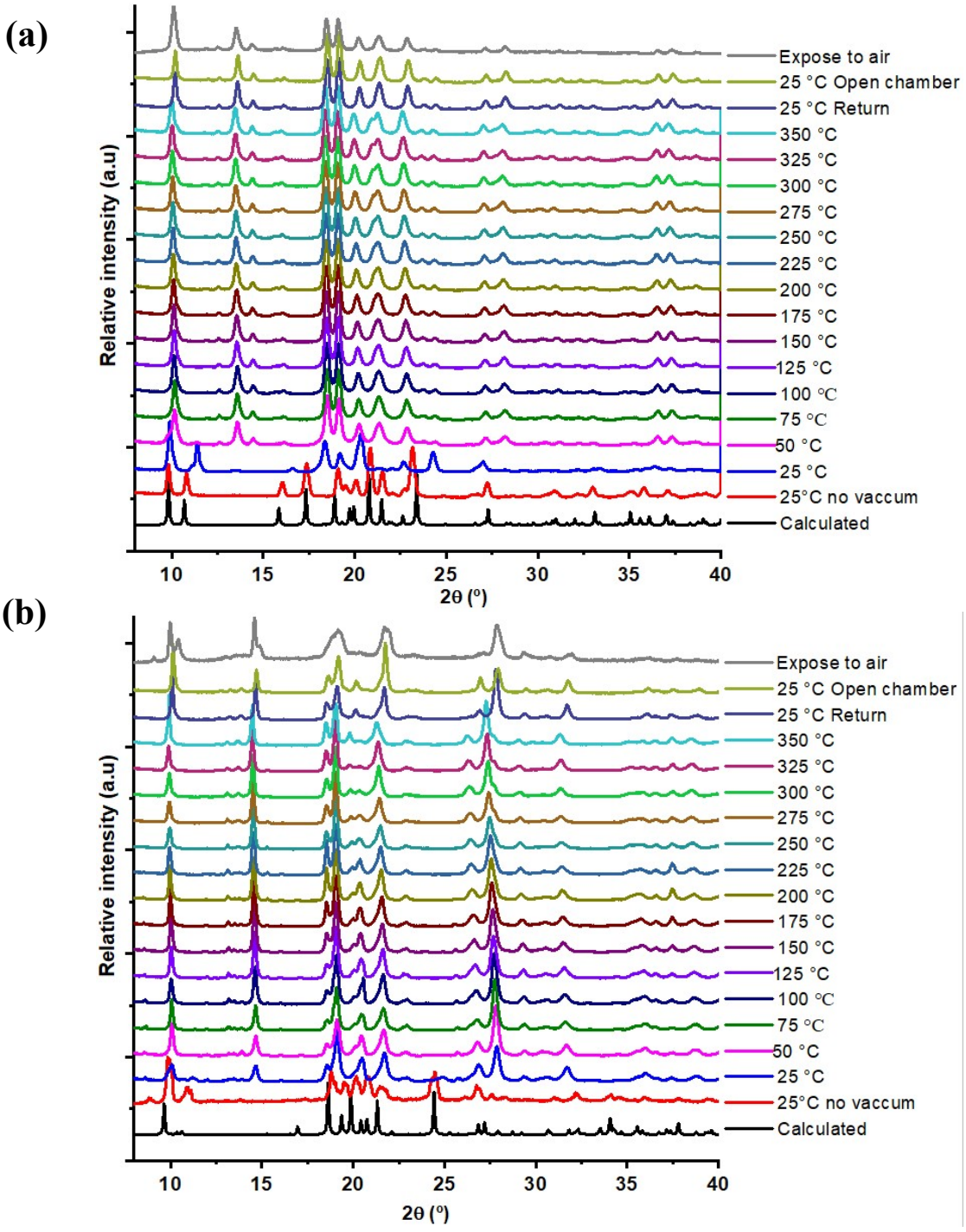

Figure S12. VT-PXRD patterns of **1** and **2** (a and b respectively) in the range 25−350 °C, returned to 25 °C under vacuum and subsequent exposure to air at room temperature.

The variable-temperature powder X-ray diffraction (VT-PXRD) patterns for **1** and **2** (see Figure 6) show that the material earlier transforms to an intermediate phase at 25 °C (under

vacuum), indicated mainly in the case of **1** (see Figure 6a) by the disappearance of the peak at 10.7, 15.9, 17.3, 20.7, 21,5 and all the peak after 30° and the appearance of the new peaks at 11.4, 18.5 and 24.3°. In the case of **2** (see Figure 6b), of the peak at 16.9° is disappeared while a new peaks at 14.7, 22.8 and 29.3° are appeared. The final phase in each material appears at 50 °C (under the vacuum), indicated mainly by the disappearance of the peaks at 11.4 and 24.3° 2θ and the appearance of the new peaks at 13.6, 14.5, 21.5, 28.4, 36.5 and 37.4° 2θ for **1** while for **2,** only the peak at 11.04° is disappeared indicating that the desolvation, both materials have different crystalline structure. The structure of **1** and **2** remain relatively crystalline up to 350 °C and remains the same after returning to 25°C. After 24h exposition to air, **1** and **2** remains unchanged.

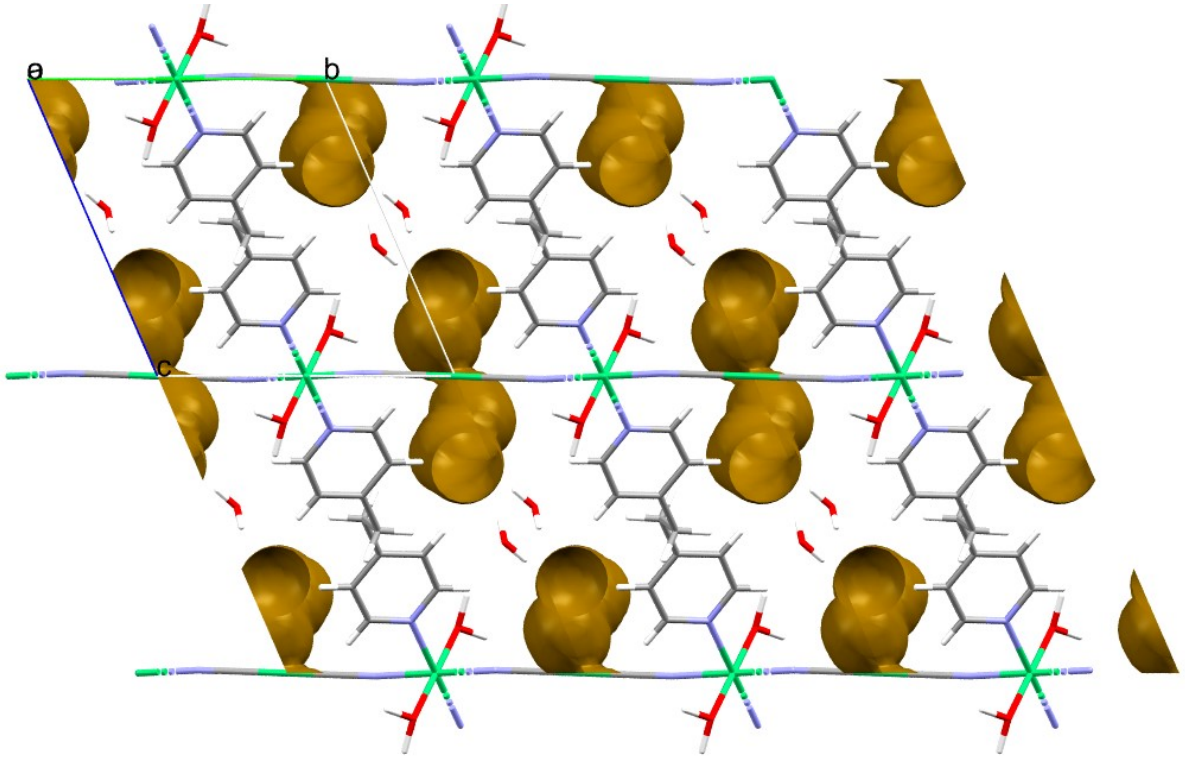

Figure S13. Potential void spaces without terminal cyanide group (the one with a disorder structure) in compound **1** as viewed along the a-axis directions.

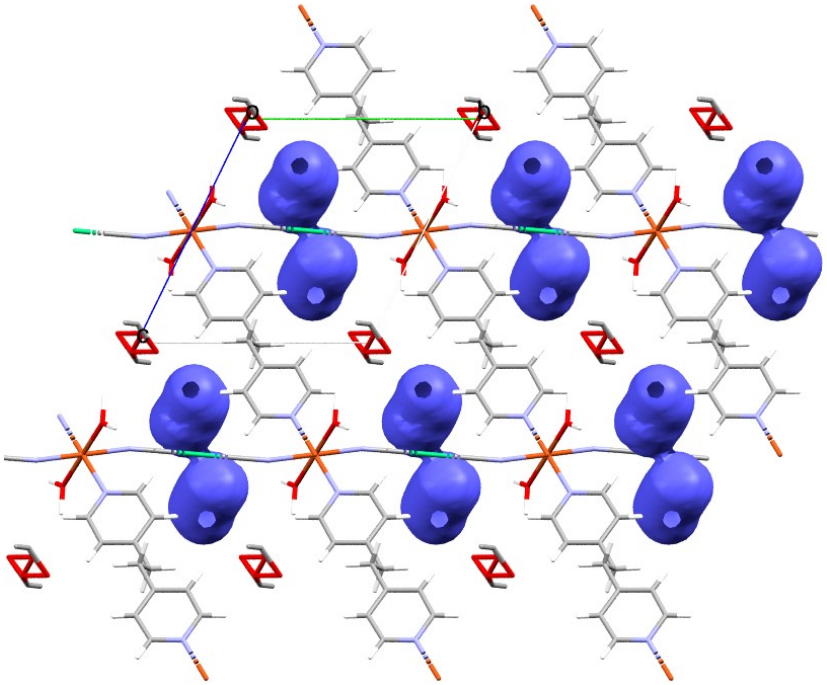

Figure S14. Potential void spaces without terminal cyanide group in compound **2**as viewed along the a-axis directions.

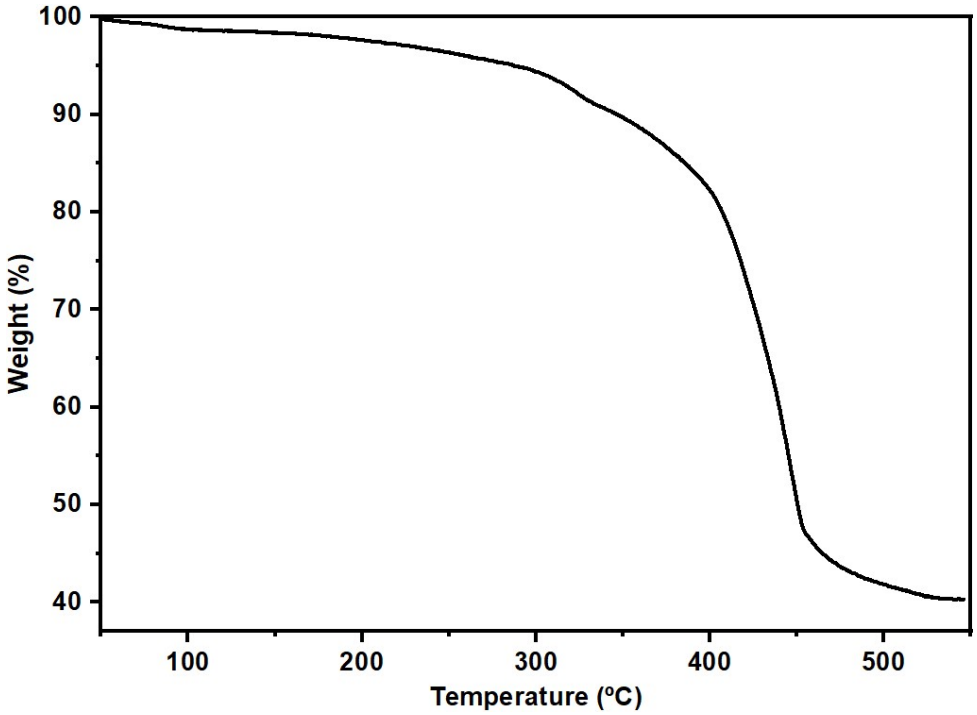

Figure S15. Thermogravimetric curve of compound **1** when dehydrated at 70°C.

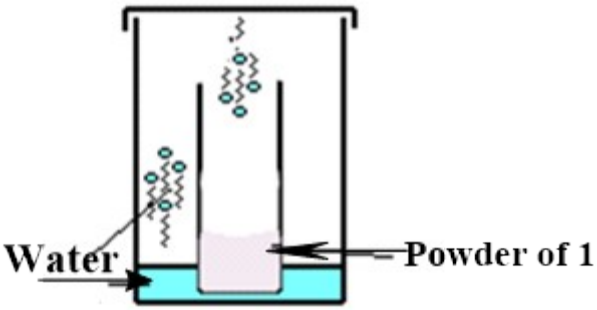

Figure S16. Diffusion system employed for the rehydration of powder of **1**.

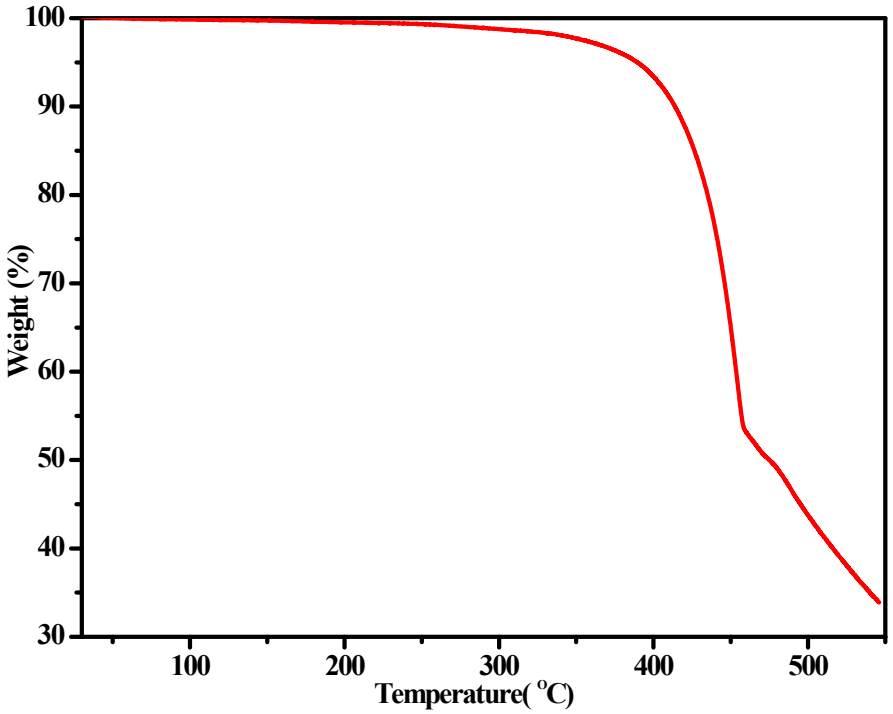

Figure S17. Thermogravimetric curve of compound 1 after exposure to air for 24 hours.

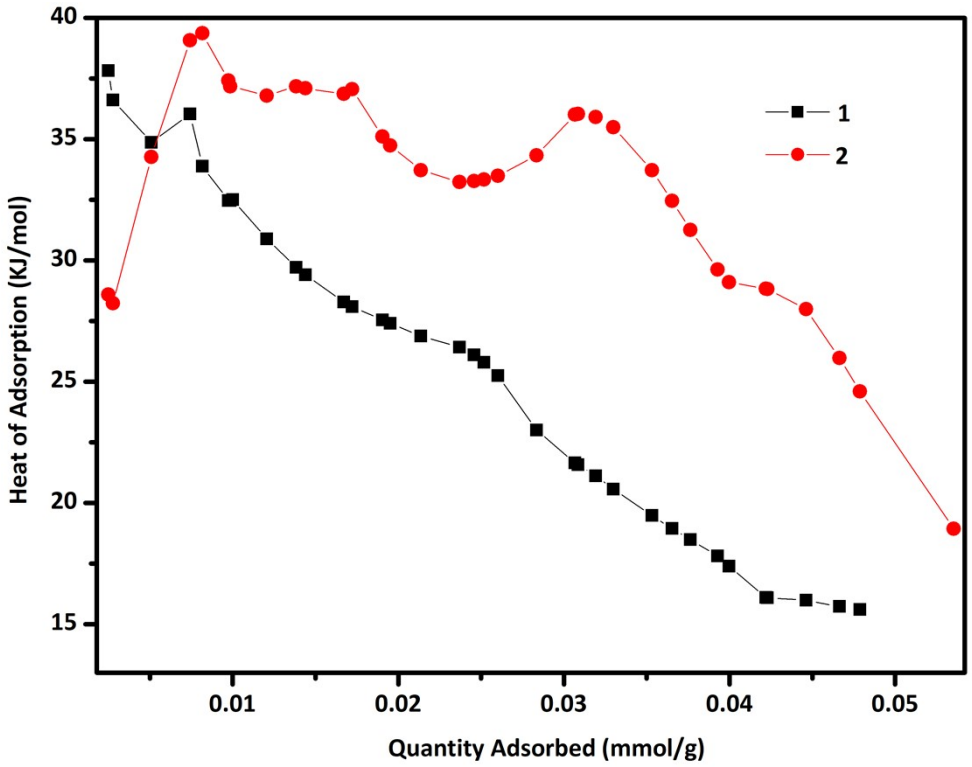

Figure S18. Heat of adsorption plot based on CO_2 isotherms from 273-298 K of **1** and **2**

Note that the maxima of load range values are determined by the maxima of 298 K isotherms for the MOF because 298 K CO_2 isotherms have the lowest sorption [9]

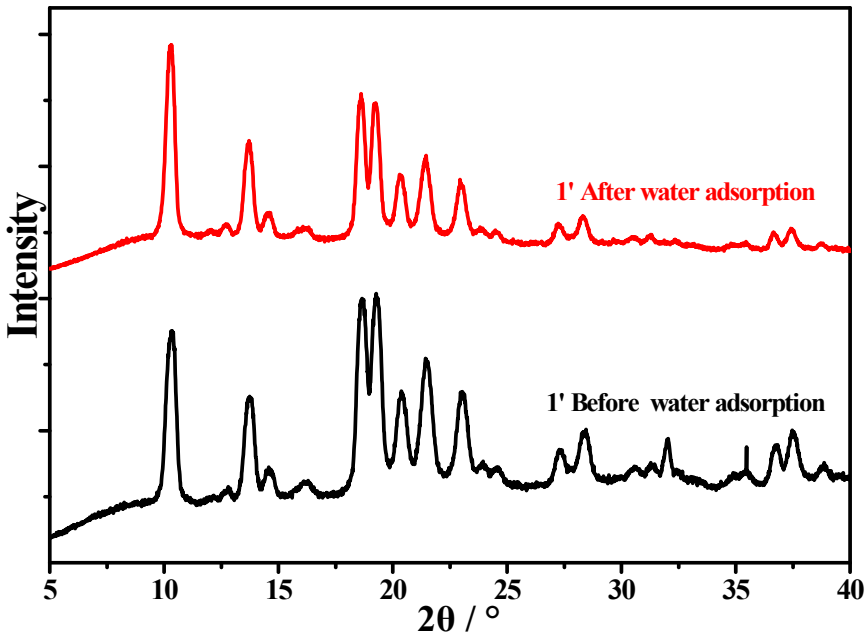

Figure S19. Powder X-ray diffraction patterns of **1** before and after water vapor adsorption analysis.

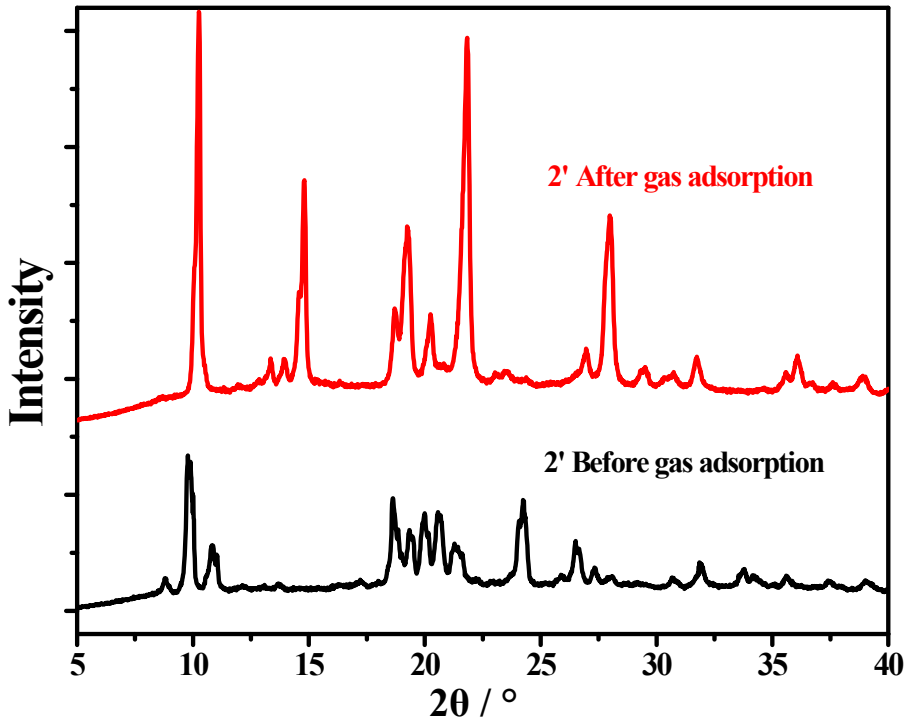

Figure S20. Powder X-ray diffraction patterns of **2** before and after water vapor adsorption analysis.

References

1. N. Vannerberg, *Acta Chem. Scand.*, 1964, **18**, 2385.
2. E. Sayın, G. S. Kürkçüoğlu, O. Z. Yeşilel and M. Taş, *J. Coord. Chem.*, 2016, **69**, 1226-1235.
3. F. Çetinkaya, G. S. Kürkçüoğlu, O. Z. Yeşilel, T. Hökelek and H. Dal, *Polyhedron*, 2012, **47**, 126-133.
4. J. Černák and K. A. Abboud, *Acta Crystallogr. C Struct. Chem Acta Commun*, 2000, **56**, 783-785.
5. W. Wong-Ng, J. T. Culp, Y.-S. Chen, J. R. Deschamps and A. Marti, *Solid State Sci.*, 2016, **52**, 1-9.
6. N. de la Pinta, S. Martín, M. K. Urtiaga, M. G. Barandika, M. I. Arriortua, L. Lezama, G. Madariaga and R. Cortés, *Inorg. Chem.*, 2010, **49**, 10445-10454.
7. M. A. Susano, P. Martín-Ramos, T. M.R. Maria, S. Folkersma, L. C. J. Pereira, and M R. Silva, J. Mol. Struct, 2017, 1147, 76-83.

8. M. A. Halim, S. Karmakar, M. A. Hamid, C. S. S. Chandan, I. Rahaman, M. E. Urena, A. Haque, M. Y. Chen, C. P. Rhodes and G. W. Beall, *ACS Appl. Mater. Interfaces*, 2023, **15**, 53568-53583.
9. N. Chatterjee and C. L. Oliver, *Inorg. Chem.*, 2022, **61**, 3516-3526.